DTIC FILE COPY

UNCLASSIFIED

(2)

AD-A196 183

DOCUMENTATION PAGE

Form Approved OMB No. 0704-0188

	1b. RESTRICTIVE MARKINGS: N/A
2a. N/A	3. DISTRIBUTION/AVAILABILITY OF REPORT: Approved for public release; distribution unlimited
2b. DECLASSIFICATION/DOWNGRADING SCHEDULE: N/A	
4. PERFORMING ORGANIZATION REPORT NUMBER(S)	5. MONITORING ORGANIZATION REPORT NUMBER(S)
6a. NAME OF PERFORMING ORGANIZATION: NAVAL RESEARCH LABORATORY Underwater Sound Reference Detach	6b. OFFICE SYMBOL (If applicable): Code 5983
6c. ADDRESS (City, State, and ZIP Code): P.O. Box 568337 Orlando, Fl 32856-8337	7a. NAME OF MONITORING ORGANIZATION
	7b. ADDRESS (City, State, and ZIP Code)
8a. NAME OF FUNDING/SPONSORING ORGANIZATION	8b. OFFICE SYMBOL (If applicable)
8c. ADDRESS (City, State, and ZIP Code)	9. PROCUREMENT INSTRUMENT IDENTIFICATION NUMBER

DTIC ELECTE JUN 03 1988 D

10. SOURCE OF FUNDING NUMBERS			
PROGRAM ELEMENT NO.	PROJECT NO.	TASK NO	WORK UNIT ACCESSION NO.
61153N	RR011-08-42	XXXXXXX	59-0589-00

11. TITLE (Include Security Classification)
Spherical-wave scattering by a finite-thickness solid plate of infinite lateral extent, with some implications for panel measurements

12. PERSONAL AUTHOR(S)
Jean C. Piquette

13a. TYPE OF REPORT	13b. TIME COVERED	14. DATE OF REPORT (Year, Month, Day)	15. PAGE COUNT
Journal Article	FROM _____ TO _____		

16. SUPPLEMENTARY NOTATION
J. Acoust. Soc. Am. 84(4), 1284-1294 (Apr 1988)

17. COSATI CODES			18. SUBJECT TERMS (Continue on reverse if necessary and identify by block number)	
FIELD	GROUP	SUB-GROUP	Acoustic scattering	Spherical waves
20	01		Reflection	Symbolic computation
			Panel measurements	

19. ABSTRACT (Continue on reverse if necessary and identify by block number)

The solution to the problem of the interaction of a spherical wave with a homogeneous and isotropic solid plate of infinite lateral extent, but finite thickness, is considered theoretically. Both the source and the plate are immersed in an infinite, inviscid fluid. Appropriate boundary conditions are imposed on the full three-dimensional elasticity equations. The solution is evaluated numerically for a variety of materials for a 1-kHz incident spherical wave and for a 5-kHz incident spherical wave. For the numerical study, the fluid medium is taken to be water. Under certain conditions, "overpressures" are predicted for both the reflected and transmitted fields (i.e., the amplitude of the reflected pressure and/or the transmitted pressure can exceed the maximum value of the amplitude of the incident pressure on the plate surface). These overpressures are consistent with the law of conservation of energy in the sense that, for a plate composed of lossless material, the total incident

(CONTINUED ON REVERSE)

20. DISTRIBUTION/AVAILABILITY OF ABSTRACT	21. ABSTRACT SECURITY CLASSIFICATION
☒ UNCLASSIFIED/UNLIMITED ☐ SAME AS RPT. ☐ DTIC USERS	UNCLASSIFIED

22a. NAME OF RESPONSIBLE INDIVIDUAL	22b. TELEPHONE (Include Area Code)	22c. OFFICE SYMBOL
Jean C. Piquette	(407) 857-5250	NRL-USRD Code 5983

DD Form 1473, JUN 86 — Previous editions are obsolete. — SECURITY CLASSIFICATION OF THIS PAGE

S/N 0102-LF-014-6603

ITEM 19-ABSTRACT CONTINUED

power is found to be equal to the sum of the total reflected power plus the total transmitted power. An important conclusion ~~of this research~~ is that the practice of attempting to reduce the influence of edge diffraction in panel tests by using samples of increasingly larger lateral extent may result in measurements that are substantially corrupted by wave-front curvature effects, particularly if the sample panel includes a steel backing plate. Keywords: → to help

Reprinted from THE JOURNAL of the Acoustical Society of America

Vol. 83, No. 4, April 1988

Spherical-wave scattering by a finite-thickness solid plate of infinite lateral extent, with some implications for panel measurements

Jean C. Piquette
Naval Research Laboratory, Underwater Sound Reference Detachment, P. O. Box 568337, Orlando, Florida 32856-8337

pp. 1284-1294

Spherical-wave scattering by a finite-thickness solid plate of infinite lateral extent, with some implications for panel measurements

Jean C. Piquette
Naval Research Laboratory, Underwater Sound Reference Detachment, P. O. Box 568337, Orlando, Florida 32856-8337

(Received 19 December 1986; accepted for publication 29 December 1987)

The solution to the problem of the interaction of a spherical wave with a homogeneous and isotropic solid plate of infinite lateral extent, but finite thickness, is considered theoretically. Both the source and the plate are immersed in an infinite, inviscid fluid. Appropriate boundary conditions are imposed on the full three-dimensional elasticity equations. The solution is evaluated numerically for a variety of materials for a 1-kHz incident spherical wave and for a 5-kHz incident spherical wave. For the numerical study, the fluid medium is taken to be water. Under certain conditions, "overpressures" are predicted for both the reflected and transmitted fields (i.e., the amplitude of the reflected pressure and/or the transmitted pressure can exceed the maximum value of the amplitude of the incident pressure on the plate surface). These overpressures are consistent with the law of conservation of energy in the sense that, for a plate composed of lossless material, the total incident power is found to be equal to the sum of the total reflected power plus the total transmitted power. An important conclusion of this research is that the practice of attempting to reduce the influence of edge diffraction in panel tests by using samples of increasingly larger lateral extent may result in measurements that are substantially corrupted by wave-front curvature effects, particularly if the sample panel includes a steel backing plate.

PACS numbers: 43.20.Fn, 43.30.Gv

LIST OF SYMBOLS

$\mathbf{A}$	vector potential in the solid
A_0	$jP_0e^{-jkz'}z'$
$a(\beta),b(\beta),c(\beta),$ $d(\beta),e(\beta),f(\beta)$	expansion functions
c_l,c_s	longitudinal speed and shear speed in the solid, respectively
$\dot{E}_i,\dot{E}_r,\dot{E}_t$	incident power, reflected power, and transmitted power, respectively
j	imaginary unit $=\sqrt{-1}$
$J_0(z),J_1(z)$	cylindrical Bessel functions of the first kind of argument z and orders 0 and 1, respectively
k	real wavenumber in the inviscid fluid surrounding the plate
k_l,k_s	complex longitudinal wavenumber and complex shear wavenumber in the solid, respectively
k_2	wavenumber in the fluid slab
l	plate thickness
p_i	incident pressure
p_r,p_t	reflected pressure and transmitted pressure, respectively
p'	a general pressure variable equal to p_i+p_r when evaluated at $z=0$, and equal to p_t when evaluated at $z=-l$.
P_0	incident spherical wave pressure amplitude coefficient; $p_i=P_0z'e^{-jkz'}e^{jkr}/r$
r,θ,z	cylindrical polar coordinates (see Fig. 1)
r'	radius of the "circle of observation" (see text for definition)
R	reflection coefficient evaluated at the origin of coordinates
T	transmission coefficient evaluated at the point $(0,0,-l)$
$\mathbf{u}$	particle displacement in the solid
z'	z coordinate of the spherical-wave source
λ,μ	Lamé parameters
ρ_1	density of the solid
$\sigma_r,\sigma_\theta,\sigma_z,$ $\tau_{\theta z},\tau_{rz},\tau_{r\theta}$	stress components
ψ	scalar potential in the solid
ω	angular frequency of the spherical wave

INTRODUCTION

Generally, the plane-wave reflection coefficient and the plane-wave transmission coefficient are the quantities of interest in panel measurements. Plane-wave conditions are often established by utilizing the farfield[1] of a source. However, due to the limited size of test facilities, it is not always practical to achieve the desired separation between the source and the test panel. Therefore, it is important to deter-

mine the potential ramifications of performing panel measurements in the nearfield[1] of a source. One of the simplest cases to consider is that of the sound radiation from a point source interacting with a single-layer, homogeneous, isotropic solid plate of infinite lateral extent but finite thickness.

The interaction of a spherical wave with a plane has long been of interest to the geophysics community.[2–6] However, the results of this previous work are not immediately applicable to panel measurements for a variety of reasons. Often, only high-frequency or farfield limiting cases have been considered. Much of this previous work has not included the influence of shear waves in the solid, or has neglected loss, or has considered only semi-infinite solid media. Rarely has a transmitted wave been computed, and generally not for the case in which the medium behind the solid (with respect to the source) is also an inviscid fluid. In order to be useful in evaluating panel measurements, one needs the *general* solution to the problem of a spherical wave interacting with a lossy, finite-thickness solid that is both homogeneous and isotropic. The source and the solid must both be immersed in an inviscid fluid medium. It is the purpose of the present article to discuss the consequences of the solution to this problem for panel measurements.

The approach taken to obtain the solution is to impose the appropriate boundary conditions on the full three-dimensional elasticity equations. Solutions to elasticity problems are rarely based on the complete elasticity theory, owing to the complexity of the attendant mathematics. However, due to the relatively recent advent of computer programs that are capable of directly manipulating mathematical symbols, this difficulty is no longer insuperable. Unlike computer languages like FORTRAN and BASIC, such symbol manipulation programs do *not* require numerical values to be assigned to the symbolic quantities of interest. Thus one can bring the full power, speed, and memory capabilities of a modern computer to bear on problems involving the manipulation of quantities containing thousands of algebraic symbols. In addition to being capable of performing the standard algebraic operations of expansion, factorization, rationalization, etc., many such programs can also perform several calculus-type operations, such as differentiation (of very complicated expressions) and integration (of somewhat elementary expressions). Of course, such programs are really only "slaves" that can perform calculations that are capable of algorithmic description, such as computing the derivative of an expression containing, say, 100 factors (a task that may be beyond human capability). However, such programs are incapable of performing tasks that require human talent, such as choosing an appropriate series expansion to satisfy both a given differential equation and the appropriate boundary conditions. They are, of course, completely incapable of choosing *which* differential equation to solve, as well as which boundary conditions are appropriate. Thus such symbol manipulators bear approximately the same relationship to the process of obtaining the solution to a physical problem as word processing programs bear to the process of creating a manuscript.

The theoretical results discussed in this article were derived with the help of the SMP™ computer program. This program also has the added benefit of being able to directly generate FORTRAN subroutines that can numerically evaluate the resulting complicated symbolic expressions. Thus, once the symbolic expressions for the boundary conditions and the assumed solutions have been defined, the process of imposing the boundary conditions on the assumed solutions is relatively straightforward. However, the problem of numerically evaluating the required integrals must still be tackled by more conventional means.

The theory is developed in Sec. I. Numerical results are presented in Sec. II. Some consequences of the theoretical results for panel measurements are given in Sec. III. Finally, a summary and the conclusions are given in Sec. IV.

I. THEORY

The theoretical approach used here is the same as that used in Ref. 1, in which the scattering of a spherical wave by an elastic cylinder is considered. However, unlike that case, the differential equations in the present problem are solved exactly. Also, unlike Ref. 1, the numerical investigation considered here includes the effects of nonzero loss in both the bulk and shear moduli of the material composing the plate

A. Differential equations

The geometry of the scattering problem and the coordinate system are presented in Fig. 1. Following the procedure of Ref. 1, we begin the present investigation by first considering the equation of motion of waves in a solid elastic medium[7]

$$(\lambda + 2\mu)\nabla(\nabla\cdot\mathbf{u}) - \mu\nabla\times(\nabla\times\mathbf{u}) = \rho_1 \frac{\partial^2 \mathbf{u}}{\partial t^2}. \qquad (1)$$

We assume that the displacement $\mathbf{u}$ in the solid can be re-

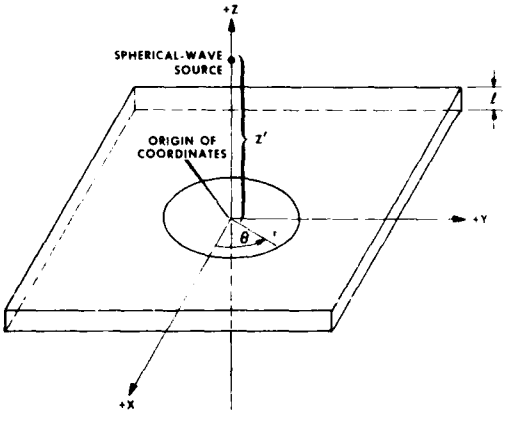

FIG. 1. A square cross section of a homogeneous and isotropic solid plate of thickness l, with infinite lateral dimensions. An infinite, inviscid fluid medium is located on both sides of the plate. A spherical-wave source is located at an offset distance z' from one side of the plate. The point of contact of the perpendicular between the spherical-wave source and the plate defines the origin of coordinates. The coordinate system is cylindrical polar, with coordinate variables r, θ, z. For clarity in defining the polar angle, a rectangular coordinate system is also depicted.

solved via the usual Helmholtz theorem into scalar and vector potentials ψ and $\mathbf{A}$, respectively, such that

$$\mathbf{u} = -\nabla\psi + \nabla\times\mathbf{A}. \tag{2}$$

Here, ψ and $\mathbf{A}$ are required to be solutions of the differential equations

$$\nabla^2\psi - \frac{1}{c_l^2}\frac{\partial^2\psi}{\partial t^2} = 0 \tag{3}$$

and

$$\nabla^2\mathbf{A} - \frac{1}{c_s^2}\frac{\partial^2\mathbf{A}}{\partial t^2} = 0. \tag{4}$$

We can rewrite Eq. (4) by expressing $\nabla^2\mathbf{A}$ in component form,[8] giving

$$\nabla^2 A_\theta - \frac{A_\theta}{r^2} + \frac{2}{r^2}\frac{\partial A_r}{\partial\theta} = -k_s^2 A_\theta, \tag{5}$$

$$\nabla^2 A_r - \frac{A_r}{r^2} - \frac{2}{r^2}\frac{\partial A_\theta}{\partial\theta} = -k_s^2 A_r, \tag{6}$$

and

$$\nabla^2 A_z = -k_s^2 A_z. \tag{7}$$

Thus the coupled set of four partial differential equations to be solved consists of Eqs. (3) and (5)–(7). Note that Eq. (3) yields the Helmholtz equation if harmonic time dependence is assumed. Note, in addition, that Eq. (7) is also a Helmholtz equation. However, Eqs. (5) and (6) are *not* Helmholtz equations. One consequence of this fact was that the problem of the scattering of a spherical wave by an elastic cylinder, considered in Ref. 1, was only solved approximately.

From the symmetry of Fig. 1, it is clear that none of the solutions to the present problem will depend on the coordinate variable θ. Hence, the terms containing a derivative with respect to this variable in Eqs. (5) and (6) are both zero. This means that these equations simplify to

$$\nabla^2 A_\theta - A_\theta/r^2 = -k_s^2 A_\theta \tag{8}$$

and

$$\nabla^2 A_r - A_r/r^2 = -k_s^2 A_r, \tag{9}$$

respectively. Thus, unlike the analogous situation arising in the case of the cylindrical scatter, the differential equations for the functions A_θ and A_r in the present problem are not coupled. However, Eqs. (8) and (9) still are not Helmholtz equations, due to the presence of the $-A/r^2$ terms in each equation. We will therefore follow the usual procedure used to solve such equations; namely, we will introduce the assumption of separation-of-variables. Since Eqs. (8) and (9) are of identical form, we need to consider in detail only one of these equations. In Eq. (8), we assume that the function A_θ is separable into functions $R(r)$, $\Theta(\theta)$, and $Z(z)$ such that $A_\theta = R(r)\Theta(\theta)Z(z)$. Substitution of this assumed form into Eq. (8) produces the separated set of equations

$$\frac{1}{Z(z)}\frac{d^2Z(z)}{dz^2} = -k^2 \tag{10}$$

$$\frac{1}{\Theta(\theta)}\frac{d^2\Theta(\theta)}{d\theta^2} = -m^2, \tag{11}$$

and

$$\frac{1}{rR(r)}\frac{d}{dr}\left(r\frac{dR(r)}{dr}\right) - \frac{m^2}{r^2} - k_z^2 - \frac{1}{r^2} = -k_s^2, \tag{12}$$

where m^2 and k_z^2 are separation constants. Equations (10) and (11) admit complex exponential and trigonometric solutions, where the separation constant m is required to be an integer by the periodicity condition associated with the coordinate variable θ. Equation (12) admits solutions that are Bessel functions of irrational order $\sqrt{1+m^2}$. However, due to the assumed independence of the solutions from the variable θ, the separation constant m must vanish. If we introduce a new constant k_w^2 such that

$$k_w^2 = k_s^2 - k_z^2, \tag{13}$$

the radial equation simplifies to

$$\frac{1}{r}\frac{d}{dr}\left(r\frac{dR(r)}{dr}\right) + \left(k_w^2 - \frac{1}{r^2}\right)R(r) = 0. \tag{14}$$

The only solution to Eq. (14) that obeys the physical requirement that $R(r)$ remain finite for $r = 0$ (see Fig. 1) is

$$R(r) = CJ_1(k_w r), \tag{15}$$

where C is an arbitrary constant. This means that the solutions for the functions A_θ and A_r can be built up out of complex exponential (or trigonometric) functions and the function J_1. This matter will be considered further in the next subsection.

B. Assumed forms for the solutions

In order to be able to solve the differential equations represented by Eq. (3) (under the assumption of harmonic time dependence) and Eqs. (7)–(9), it is first worthwhile to choose an appropriate expansion for the incident spherical wave. This is[9]

$$p_i = A_0\int_0^\infty \frac{J_0(\beta r)\exp[j\sqrt{k^2-\beta^2}(z'-z)]}{\sqrt{k^2-\beta^2}}\beta\,d\beta, \tag{16}$$

which is valid for $z < z'$.

In constructing the solutions to the present problem, it is important to note that this process is greatly simplified in the present case since all such solutions can be expressed in terms of standard wavefunctions. It is also important to take cognizance of the symmetry of the problem. In the present case, symmetry requires the solutions to be independent of the θ coordinate. Also, it is important to bear in mind the boundary conditions that must be satisfied. These will be considered in the next subsection. We will therefore proceed to assume that the solutions to the present problem may be expressed in the form

$$p_r = \int_0^\infty \frac{a(\beta)J_0(\beta r)\exp[-j\sqrt{k^2-\beta^2}(z'-z)]\beta\,d\beta}{\sqrt{k^2-\beta^2}}, \tag{17}$$

$$p_r = \int_0^\infty \frac{a(\beta)J_0(\beta r)\exp[-j\sqrt{k^2-\beta^2}(z'-z)]\beta\, d\beta}{\sqrt{k^2-\beta^2}}, \tag{17}$$

$$\psi = \int_0^\infty \frac{J_0(\beta r)\{c(\beta)\exp[j\sqrt{k_l^2-\beta^2}(z'-z)] + d(\beta)\exp[-j\sqrt{k_l^2-\beta^2}(z'-z)]\}\beta\, d\beta}{\sqrt{k_l^2-\beta^2}}, \tag{19}$$

$$A_\theta = \int_0^\infty \frac{J_1(\beta r)\{e(\beta)\exp[j\sqrt{k_s^2-\beta^2}(z'-z)] + f(\beta)\exp[-j\sqrt{k_s^2-\beta^2}(z'-z)]\}\beta\, d\beta}{\sqrt{k_s^2-\beta^2}}, \tag{20}$$

and $A_z = A_r = 0$. Here, a, b, c, d, e, and f are six unknown functions to be determined.

Of course, in order to justify these assumed forms, two conditions must be satisfied. First, they must represent particular solutions of the partial differential equations. Second, they must be capable of satisfying all the boundary conditions involved in the physical problem. We take up the latter point in the next subsection.

To see that the given assumed forms do in fact satisfy the differential equations, note first that the quantities p_r and p_t represent pressure waves in the fluid surrounding the solid. Therefore, the differential equation that governs the behavior of these functions is the Helmholtz equation. Equations (17) and (18) are clearly particular solutions of the Helmholtz equation because they are constructed from standard wavefunctions. [Note also the similarity of Eqs. (17) and (18) to the expansion for p_t given in Eq. (16).] The same argument applies to the expansion for the function ψ, given in Eq. (19), since this function's governing differential equation, Eq. (3), is also a Helmholtz equation, under the assumed harmonic time dependence. The solution for A_θ has been constructed to be consistent with the discussion given in connection with Eqs. (10)–(15). Hence, Eq. (20) is seen to be a particular solution of Eq. (8). Finally, note that the equations $A_z = A_r = 0$ are the trivial solutions to Eq. (7) and Eq. (9), respectively. Thus it only remains to be shown that these assumed forms can satisfy the boundary conditions of the problem. We consider this matter next.

C. Boundary conditions

There are three boundary conditions for the present problem, each of which must be imposed at each of the two fluid–solid interfaces. [This explains why six unknown expansion functions a–f are needed to formulate the assumed solutions represented by Eqs. (17)–(20).] These three boundary conditions are: (i) the continuity of normal displacement, (ii) the continuity of normal stress, and (iii) the vanishing of shear stress. By combining the general expression for strain written in cylindrical coordinates[10] with Hooke's law for isotropic media,[11] we obtain the stress–strain relationships

$$\sigma_r = 2\mu\frac{\partial u_r}{\partial r} + \lambda\nabla\cdot\mathbf{u}, \tag{21}$$

$$\sigma_\theta = \frac{2\mu}{r}\frac{\partial u_\theta}{\partial\theta} + \lambda\nabla\cdot\mathbf{u}, \tag{22}$$

$$\sigma_z = 2\mu\frac{\partial u_z}{\partial z} + \lambda\nabla\cdot\mathbf{u}, \tag{23}$$

$$\tau_{\theta z} = \mu\left(\frac{\partial u_z}{r\partial\theta} + \frac{\partial u_\theta}{\partial z}\right), \tag{24}$$

$$\tau_{zr} = \mu\left(\frac{\partial u_r}{\partial z} + \frac{\partial u_z}{\partial r}\right), \tag{25}$$

and

$$\tau_{r\theta} = \mu\left(\frac{\partial u_\theta}{\partial r} - \frac{u_\theta}{r} + \frac{1}{r}\frac{\partial u_r}{\partial\theta}\right). \tag{26}$$

It is next helpful to reexpress the stress components in terms of the potentials $\mathbf{A}$ and ψ. This may be done with the help of Eq. (2). Also, it should be noted that attempting to directly impose the boundary conditions will result in a set of equations that is difficult to solve. A more convenient set of equations is obtained if the equation that imposes continuity of normal displacement is differentiated with respect to r. (This is a legitimate operation because, although this equation is evaluated at a particular value of z, it must hold for all values of r. Hence, each side of the equation is a continuously differentiable function of r.) Equation (8) can be used to replace combinations of terms in the boundary condition equations with simplified expressions. If we also utilize the symmetry requirement that the solutions be independent of θ, and if we further take advantage of the assumption that $A_z = A_r = 0$, the boundary conditions assume the form

$$\frac{1}{\rho_0\omega^2}\frac{\partial^2 p'}{\partial z\,\partial r} = \left(-\frac{\partial^2\psi}{\partial r\,\partial z} - k_s^2 A_\theta - \frac{\partial^2 A_\theta}{\partial z^2}\right) \tag{27}$$

(for the continuity of normal displacement),

$$p' = -\left(-2\mu\frac{\partial^2\psi}{\partial z^2} + \lambda k_l^2\psi\right) \tag{28}$$

(for the continuity of normal stress), and

$$0 = \mu\left(-2\frac{\partial^2\psi}{\partial z\,\partial r} - 2\frac{\partial^2 A_\theta}{\partial z^2} - k_s^2 A_\theta\right) \tag{29}$$

(for the vanishing of shear stress).

Note that Eqs. (27)–(29) are written so that the left-hand sides refer to the fluid and the right-hand sides refer to the solid [e.g., the left-hand side of Eq. (28) represents the stress in the fluid, while the right-hand side of this equation represents the normal stress in the solid]. Each of these boundary conditions must be imposed both at $z = 0$ and $z = -l$ (refer to Fig. 1). The integral equations that result from substituting Eqs. (16)–(20) into the boundary conditions of Eqs. (27)–(29) can be converted into algebraic equations by using the orthogonality property of the Bessel function. This results in a set of six algebraic equations in the six unknown functions a–f. As previously remarked, this procedure was implemented with the help of the symbolic manipulation computer

program SMP. This program was also used to analytically solve the resulting algebraic set, and to generate FORTRAN subroutines that permit numerical evaluation of the expansion functions $a(\beta)$ and $b(\beta)$.

Note that, since the algebraic set of six equations in the six functional unknowns a–f is capable of analytical solution, this completes the demonstration that the assumed forms of the solutions, given by Eqs. (17)–(20), are appropriate for the present problem. The resulting analytical solutions for the expansion functions are extremely complicated and unwieldy, and are not particularly illuminating. Therefore, we will not display the analytical expressions, and will choose instead to investigate several numerical examples.

II. NUMERICAL CALCULATIONS

Preliminary plots of the real and imaginary parts of the integrands containing the expansion functions $a(\beta)$ and $b(\beta)$ revealed variations [for the materials and frequency interval of interest (1–5 kHz)] that are similar to the variations observed in the expansion functions of Ref. 1. Namely, the integrands vary slowly over most of the integration interval, but can have large fluctuations about a small number of points (see Fig. 3 of Ref. 1). Hence, a similar numerical scheme was applicable in the present case for evaluating the integrals of Eqs. (17) and (18). (These equations give representations of the reflected pressure and the transmitted pressure, respectively.) In summary, the numerical scheme involves first splitting the infinite integration interval into a finite subinterval plus an infinite subinterval. The finite subinterval is then searched for the regions of most-rapid variation of the integrand. The integral over the finite subinterval is then evaluated using a Gauss–Legendre[12] numerical integration procedure, with the greatest density of quadrature points being located in the regions of most-rapid variation of the integrand. The small contribution to the total integral from the infinite subinterval is then evaluated using a 15-point Gauss–Laguerre[13] numerical integration procedure. See Ref. 1 for a more detailed description of the numerical integration process.

As was the case for the solution presented for the expansion function in Ref. 1, the solutions for the expansion functions in the present problem are extremely complicated. However, since the analytical solutions and the required FORTRAN subroutines for evaluating them numerically were obtained using a symbolic computation program, the likelihood of mathematical slips occurring in obtaining the solutions, and in generating the required computer programs to numerically evaluate the results, is considerably reduced. Nonetheless, it is important to investigate limiting test cases to gain confidence in the reliability of the software before venturing into calculations of a more general (and more interesting) nature.

A very useful test case is the problem of the interaction of a spherical wave with a finite-thickness fluid plane. As is the case for the solid, an infinite, inviscid fluid medium is located on both sides of the fluid plane. (The two fluids involved in this reduced problem are of course assumed to be immiscible.) The solution to this problem is relatively straightforward to obtain by analogy to the solution to the related problem involving an incident plane wave.[14]

The functional expansions introduced for the incident, reflected, and transmitted waves for the purpose of obtaining the solution to the general problem [i.e., Eqs. (16)–(18), respectively] are also applicable to the finite-thickness fluid plane problem. For the waves *internal* to the fluid plane, the following expansion is also useful[15]:

$$p_{\text{int}} = \int_0^\infty \frac{J_0(\beta r)\{g(\beta)\exp[j\sqrt{k_2^2-\beta^2}\,(z'-z)] + h(\beta)\exp[-j\sqrt{k_2^2-\beta^2}\,(z'-z)]\}\beta\, d\beta}{\sqrt{k_2^2-\beta^2}}. \tag{30}$$

In Eq. (30), k_2 denotes the wavenumber in the fluid composing the plane, and g and h are functions to be determined. [Of course, the functions a and b of Eqs. (17) and (18) are also unknowns that must be redetermined for the present case.] The boundary conditions for the finite-thickness fluid plane problem are: (i) the continuity of normal displacement and (ii) the continuity of pressure. Each of these conditions must be evaluated both at $z = 0$ and at $z = -l$. This explains why four unknown expansion functions a, b, g, and h are required in the representations of the solutions for the reduced problem.

The solution to the fluid plane problem described above was also implemented using the SMP symbolic computation program. The same subroutine that was used to numerically evaluate the integrals required to compute the reflected-wave pressure and the transmitted-wave pressure in the more general case was also used to evaluate the associated integrals arising in the reduced problem. The resulting computer program was then used to evaluate reflected and transmitted waves arising from a spherical wave interacting with a finite-thickness fluid plane. Calculations were performed for a variety of fluid properties and for test frequencies 1 and 5 kHz. The fluid properties chosen do not correspond to those of any real fluids, but rather are representative of the densities and sound speeds characteristic of the solids of interest (i.e., metals and elastomers). The density range of the fictitious fluids considered was 0.5–0.8 g/cm^3. The sound-speed range considered was 1.5×10^5–7.0×10^5 cm/s.

The results were next compared to numerical solutions obtained using a much simpler computer program that implements the solution to the associated problem involving the interaction of a normally incident plane wave with a fluid plane. The comparison was achieved by first computing the reflected-wave pressure at the point $r = 0$, $z = 0$ for the case of the incident spherical wave. The transmitted wave pressure at the point $r = 0$, $z = -l$ was also computed for this case. The results so obtained were compared to the corresponding results obtained using plane-wave theory, evaluat-

ed at the relevant surfaces. In all cases considered, the spherical-wave solution differed very little from the plane-wave solution. For example, consider an incident spherical wave of 1-kHz frequency, originating from a source located at $z' = 200$ cm, interacting with the fictitious fluid having density 1.2 g/cm^3, sound speed 3×10^5 cm/s, and 1-cm thickness. In this case, the spherical-wave reflection coefficient, evaluated on the surface of the fluid plane that is facing the source and normalized to the incident wave at the origin of coordinates, is $9.33\times10^{-4}-2.35\times10^{-2}j$, while that for the plane wave is $6.12\times10^{-4}-2.08\times10^{-2}j$. The spherical-wave transmission coefficient for this case, evaluated on the surface of the fluid plane that is opposite the source and also normalized to the incident wave at the origin of coordinates, is. $0.993 + 2.97\times10^{-2}j$, while that for the plane wave is $0.994 + 2.93\times10^{-2}j$.

Next, the computer program that implements the solution to the full elasticity problem was used to evaluate the reflected and transmitted waves arising from the interaction of a spherical wave with a finite-thickness fluid plane. In order to do this, an extremely small value (10^{-6} dyn/cm^2) for the shear modulus μ was used. In all cases tested, the results obtained using the general computer program agreed with those obtained using the specialized computer program for this problem to within the precision of implementation.

Taking the above consistencies as indicating that the computer program that implements the general solution does not contain simple programming errors, cases were next considered which involved a solid plate. The results of several representative calculations are given in Table I. The first column of this table gives the material considered. The second column gives the frequency considered. The third through sixth columns present reflection coefficients (R) and transmission coefficients (T) for both the spherical-wave and plane-wave cases. (The coefficients are normalized to the incident wave at the origin of coordinates.) The reflection coefficients are evaluated at $r = 0$, $z = 0$ and the transmission coefficients are evaluated at $r = 0$, $z = -1$ cm. Plate thickness in all cases considered is $l = 1$ cm. Spherical-wave source offset is $z' = 200$ cm in all cases. The shear-wave speed for each material is listed for reference in the last column of the table.[16]

Note that for several of the spherical-wave cases presented, the amplitude of the reflected and/or transmitted waves exceeds that of the incident wave evaluated at the origin of coordinates. Although this unexpected result would be indicative of error in a normal-incidence plane-wave calculation, this is not necessarily so for an incident spherical wave, since the reflected and transmitted pressure amplitudes will each vary with r in this case. Nonetheless, one is reluctant to accept the validity of such computed "overpressures" without further investigation.

In order to determine whether the unexpected results of Table I might have possibly arisen from either numerical errors or computer programming errors, an energy-conservation analysis was performed. This calculation involved numerically performing the power integral[17]

$$\dot{E} = \frac{1}{2}\,\mathrm{Re}\int_0^r p^*(\mathbf{r})\mathbf{v}(\mathbf{r})\cdot\hat{n}(2\pi r\,dr). \tag{31}$$

The asterisk in Eq. (31) denotes complex conjugate. This integral was evaluated over both the front and back surfaces of the plate, and the result was compared to the total power incident on the infinite plate. (The total incident power is equal to one-half the total power radiated by the point source.) The particle velocity $\mathbf{v}$ required in Eq. (31) was evaluated numerically at each point of integration by using the gradient of the appropriate pressure term. [In essence, the partial derivative with respect to z of Eq. (17) was used to compute the required component of the particle velocity associated with the reflected pressure, and this same derivative of Eq. (18) was used to compute the required component of the particle velocity associated with the transmitted pressure. The exact relationship between each pressure gradient and the relevant particle velocity is provided by Euler's equation.] The integral of Eq. (31) was performed by using a 32-point Gauss–Legendre quadrature scheme.[12] Each of the required pressures and velocities was evaluated at each of the 32 quadrature points. Since each required velocity and pressure is defined in terms of an integral, each power calcu-

TABLE I. Spherical-wave complex reflection coefficients R and transmission coefficients T compared to plane-wave coefficients for a variety of materials, each of $l = 1$-cm thickness. PMM denotes polymethylmethacrylate. The fluid medium is water. Spherical-wave source offset z' in each case is 200 cm. R is evaluated at the origin of coordinates. T is evaluated at the point $(0,0,-l)$. Each coefficient is normalized to the incident wave evaluated at the origin of coordinates. (See Fig. 1.)

	Frequency (kHz)	R		T		Shear speed (cm/s)
		Spherical wave	Plane wave	Spherical wave	Plane wave	
Aluminum	1	$-0.482 + 0.140j$	$0.003 - 0.056j$	$1.50 - 0.223j$	$0.997 + 0.057j$	2.98×10^5
Brass	1	$-0.078 + 0.204j$	$0.031 - 0.172j$	$1.02 - 0.350j$	$0.969 + 0.173j$	2.11×10^5
Lead	1	$0.104 - 0.185j$	$0.053 - 0.223j$	$0.896 + 0.185j$	$0.947 + 0.225j$	6.98×10^4
PMM	1	$-0.174 + 1.15j$	$0.001 - 0.019j$	$0.792 + 1.18j$	$0.999 + 0.030j$	1.34×10^5
Steel	1	$-0.616 - 1.07j$	$0.025 - 0.157j$	$1.69 + 1.02j$	$0.974 + 0.157j$	3.28×10^5
Aluminum	5	$-0.133 - 0.063j$	$0.074 - 0.260j$	$0.355 + 0.562j$	$0.925 + 0.264j$	2.98×10^5
Brass	5	$1.17 - 0.614j$	$0.442 - 0.495j$	$1.22 - 0.002j$	$0.558 + 0.498j$	2.11×10^5
Lead	5	$0.575 - 0.457j$	$0.584 - 0.488j$	$0.420 + 0.468j$	$0.415 + 0.498j$	6.98×10^4
PMM	5	$0.096 - 0.237j$	$0.014 - 0.094j$	$1.03 - 0.001j$	$0.983 + 0.149j$	1.34×10^5
Steel	5	$0.625 + 0.936j$	$0.394 - 0.049j$	$0.015 - 0.844j$	$0.605 + 0.489j$	3.28×10^5

lation thus involved 65 numerical integrations (32 velocity integrals, 32 pressure integrals, and 1 integral for the calculation of the power). Of course, the integral of Eq. (31) should actually be performed for the upper limit $r' \to \infty$. However, if a sufficiently large value for r' is chosen, the vast majority of the power will be included.

Table II presents results of the power calculations for the 1-kHz case involving a steel plate of 1-cm thickness. Note from the spherical-wave values listed in Table I that the pressure amplitude of the reflected wave exceeds that of the incident wave by more than 23% in this case. The transmitted-wave pressure amplitude is nearly twice that of the incident wave. Hence, this is a particularly severe case to examine.

In Table II, the first column gives the upper limit of integration r' used in evaluating the integral of Eq. (31). It represents the radius of a circle drawn on either side of the plate having its center either (i) at the origin of coordinates (on the side of the plate facing the source) or (ii) at the point $(0,0,-l)$ (on the side of the plate opposite the source). One such circle may be taken to be that illustrated in Fig. 1, if the r coordinate is taken to be equal to r'. For the purposes of the following discussion, we will refer to either of these circles as a "circle of observation."

The quantity $\dot{E}_i(r')$ represents the power contained in that portion of the incident wave which strikes the infinite plate within the circle of observation depicted in Fig. 1. The quantity $\dot{E}_r(r')$ denotes the power contained in that portion of the reflected wave that also passes through the circle of observation on the side of the plate facing the source. Similarly, the quantity $\dot{E}_t(r')$ denotes the power contained in that portion of the transmitted wave that passes through the circle of observation on the side of the plate that is opposite the source. All values are expressed as a percentage of the total power incident on the infinite plate. The power balance can be determined by summing the values in the $\dot{E}_r(r')$ and $\dot{E}_t(r')$ columns, and comparing the result to 100% (the total incident power). The sum $\dot{E}_r(r') + \dot{E}_t(r')$ is given in the last column of Table II. As can be seen, the total never exceeds 100%. The 10 000-cm radius considered in Table II is the greatest value that could be accommodated by the numerical scheme used to evaluate the required integrals. It should be noted that this radius accounts for 98.4% of the total incident power.

By comparing the values in the $\dot{E}_i(r')$ column of the table with the values in the column that gives the sum of $\dot{E}_r(r')$ and $\dot{E}_t(r')$, it becomes clear that the power required to create the computed overpressures is provided by power contained in portions of the incident spherical wave that strike the plate in regions that are *outside the circle of observation*. This conclusion follows from the fact that the sum $\dot{E}_r(r') + \dot{E}_t(r')$ is always greater than $\dot{E}_i(r')$, although the difference $\{[\dot{E}_r(r') + \dot{E}_t(r')] - \dot{E}_i(r')\}$ clearly appears to approach zero as $r' \to \infty$. Thus the additional power arrives at the observation point either by propagating, within the plate material, from regions outside of this circle to regions interior to it, and then being reradiated into the fluid, or by direct radiation into the fluid by regions of the plate that are outside of this circle. Of course, both of these alternatives may contribute to the phenomenon. These unexpected results appear to be a consequence of solving the full three-dimensional elasticity theory. Several attempts which were considered to explain these overpressures using simplified theories were unsuccessful.[18,19] (For example,[20] the flexural-wave coincidence frequency for the steel case considered is approximately 23.7 kHz.)

We can gain further understanding of how it is possible for overpressures to be present and yet for energy to nonetheless be conserved by investigating the radial dependence of the reflected and transmitted pressures. Three cases are considered in Figs. 2 and 3.

Figure 2(a)–(c) presents reflected-wave pressure amplitudes as a function of r, evaluated at $z = 0$ and $z = 150$ cm, for steel, polymethylmethacrylate, and lead samples of 1-cm thickness, respectively. Source offset is $z' = 200$ cm and source frequency is 1 kHz. Figure 3(a)–(c) presents transmitted-wave results for these same cases, except that the patterns are evaluated at $z = -1$ cm and $z = -151$ cm. As can be seen, each of these cases has an associated beam pattern. Therefore, although the reflected and/or transmitted wave pressure amplitudes can exceed that of the incident wave in the vicinity of $r = 0$, these pressure amplitudes eventually drop below that of the incident wave at greater values of r. Thus it is not unreasonable that the integrated power over both sides of the plate can be equal to the total incident power, even though the reflected and/or transmitted wave pressure amplitudes exceed that of the incident wave in certain limited regions.

Taking this power calculation as sufficient for establishing the validity of the present results, we next investigate a possible cause of the computed overpressures. The results presented in Table I tend to support the notion that the effect is associated with the nonzero shear-wave speed associated with solids. (A similar conclusion was reached in Ref. 1 concerning a cylindrical scatterer.) Evidence for this is provided by first noting the small difference between the spherical-wave and plane-wave results presented for lead in Table I. (Note that the shear speed of lead is about one-half the sound speed in water.) Since lead has a relatively low shear speed, this minor difference between the spherical-wave results and the plane-wave results may be primarily attributable to the simple phase and amplitude variation of the incident wave across the plate surface, rather than being due to a significant shear effect. (Recall also the close agreement

TABLE II. Power balance for a 1-kHz spherical wave originating from a source located at $z' = 200$ cm and interacting with a steel plate of 1-cm thickness and infinite lateral extent. $\dot{E}_i(r')$—power incident on the relevant "circle of observation" (radius r'); $\dot{E}_r(r')$—power reflected through the relevant circle of observation; $\dot{E}_t(r')$—power transmitted through the relevant circle of observation. Results are expressed as a percentage of the total power incident on the infinite plate.

r'(cm)	$\dot{E}_i(r')$	$\dot{E}_r(r')$	$\dot{E}_t(r')$	$\dot{E}_r(r') + \dot{E}_t(r')$
100	10.5	4.18	17.1	21.3
250	37.5	15.8	24.2	40.0
1000	80.3	51.4	31.0	82.4
10 000	98.4	62.8	37.0	99.8

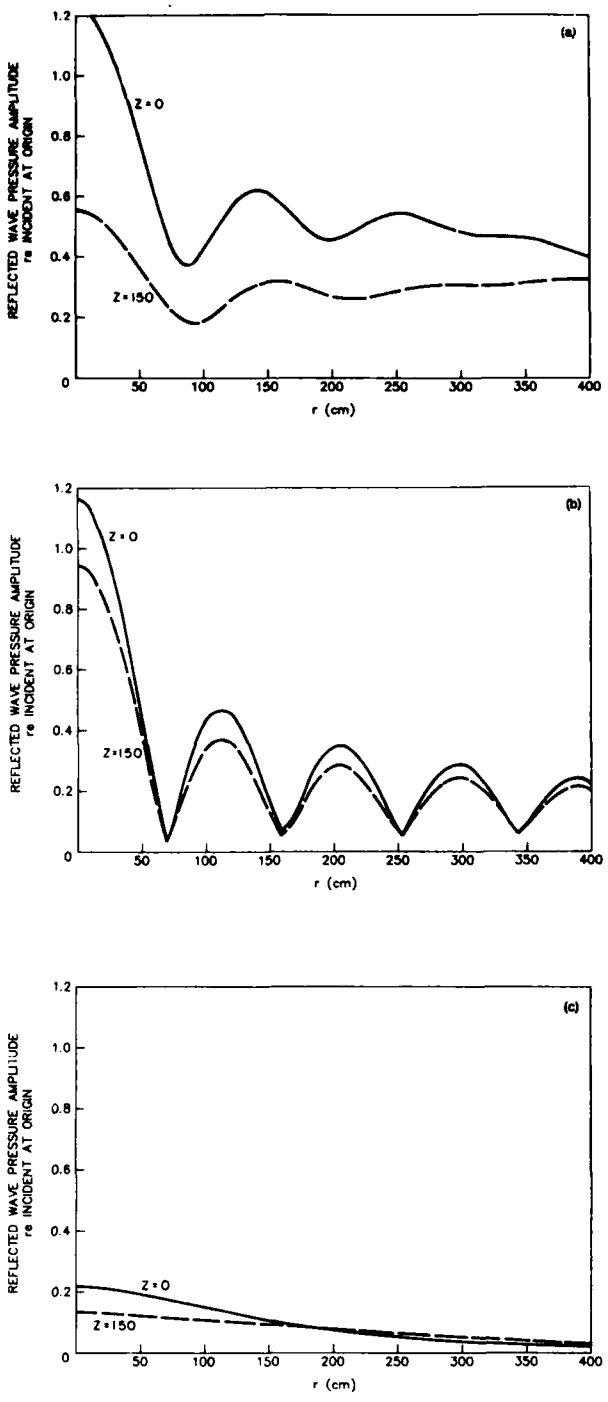

FIG. 2. Reflected-wave pressure amplitude, as a function of r, resulting from a 1-kHz incident spherical wave originating from a source located at $z' = 200$ cm. Solid line: $z = 0$; dashed line: $z = 150$ cm; sample thickness: 1 cm. Incident wave at $r = 0, z = 0$ is taken to be of amplitude 1.0: (a) steel; (b) polymethylmethacrylate; (c) lead.

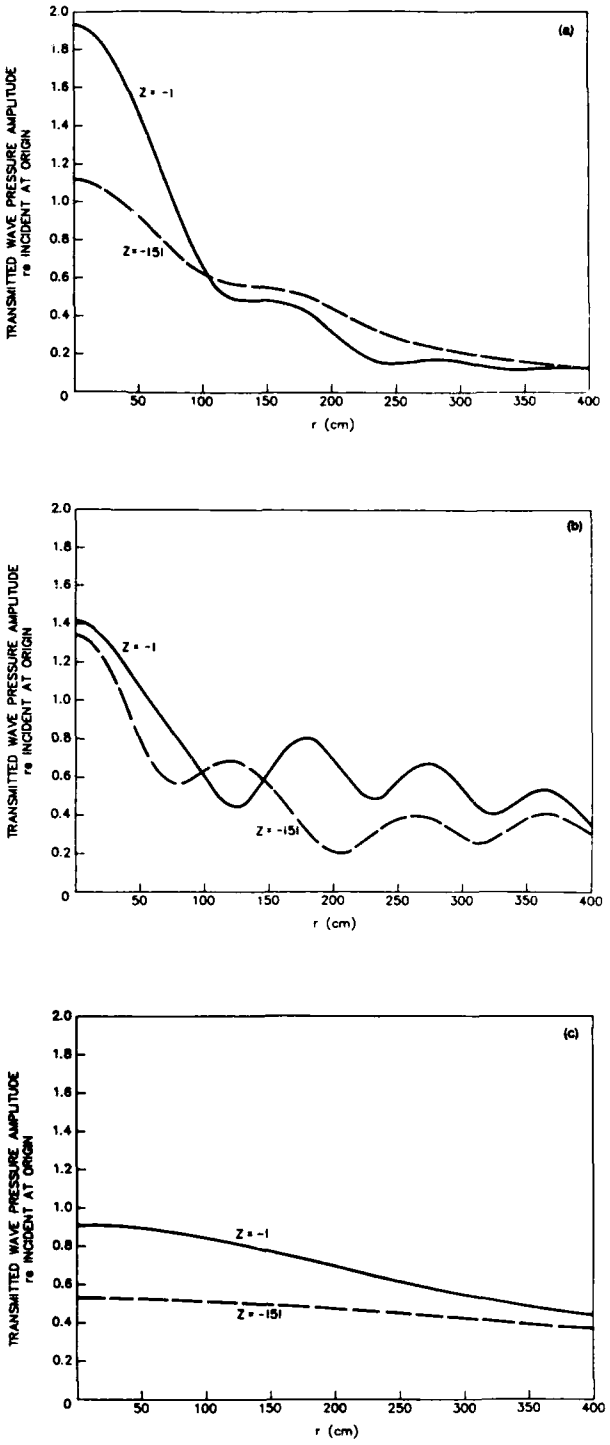

FIG. 3. Transmitted-wave pressure amplitude, as a function of r, resulting from a 1-kHz incident spherical wave originating from a source located at $z' = 200$ cm. Solid line: $z = -1$ cm; dashed line: $z = -151$ cm; sample thickness: 1 cm. Incident wave at $r = 0, z = 0$ is taken to be of amplitude 1.0: (a) steel; (b) polymethylmethacrylate; (c) lead.

between spherical-wave theory and plane-wave theory for the case of the fluid scatterer discussed earlier.) Note, however, for the materials having shear speed comparable to or significantly greater than the sound speed in water, the differences between plane-wave and spherical-wave results are much more pronounced.

We further investigate the notion that the computed

overpressures are associated with the influence of shear effects in Fig. 4(a) and (b). In these figures, the reflected and transmitted wave pressure amplitudes, evaluated on the relevant surfaces of the plate, are evaluated for a continuum of fictitious materials. As with the previous figures, the pressure amplitudes are normalized to that of that incident wave at the origin of coordinates. Each of these fictitious materials is taken to have the same density and the same longitudinal wave speed as that of steel. However, the shear modulus is allowed to vary between zero, at the left end of the abscissa, and the true shear modulus of steel, at the right end of the abscissa. (The shear modulus is normalized to that of steel, μ_s, so that the abscissa runs from 0 to 1.) Note that the pressure amplitude corresponding to $\mu/\mu_s = 0$ in each of these figures is less than the incident wave pressure amplitude at the origin of coordinates, but that this no longer holds true as μ/μ_s departs from zero. It is interesting to note that the departure of the results from those at $\mu/\mu_s = 0$ is nonmonotonic, and that there are significant intervals for which the computed pressures are significantly *less* than those expected from plane-wave theory. (The values presented for $\mu/\mu_s = 0$ do not differ significantly from the plane-wave results.)

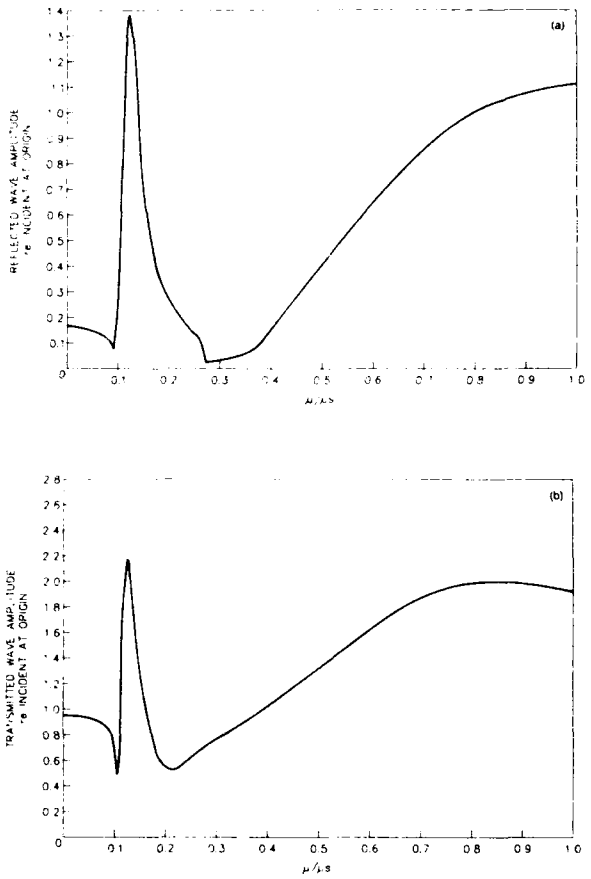

FIG. 4. Reflected- and transmitted-wave pressure amplitudes arising from an incident spherical wave, as a function of normalized shear modulus, for a continuum of fictitious quasisteel samples. The quantity μ_s denotes the shear modulus of steel. For all cases, the longitudinal wave speed in the sample is held fixed at the true value for steel. Thus $\mu/\mu_s = 0.0$ corresponds to a fictitious fluid sample having the same sound speed as the longitudinal wave speed in actual steel, and $\mu/\mu_s = 1.0$ corresponds to actual steel. Sample thickness: 1 cm; source offset: 200 cm; frequency: 1 kHz: (a) reflected-wave pressure amplitude, evaluated at $r = 0$, $z = 0$; (b) transmitted-wave pressure amplitude, evaluated at $r = 0$, $z = -1$ cm.

III. SOME CONSEQUENCES FOR PANEL MEASUREMENTS

When an unexpected result such as that reported here is obtained, one is always concerned that the "phenomenon" may be a consequence of mathematical errors or computer programming errors. However, it would be rather surprising if such errors yielded results that are consistent with the law of conservation of energy. Also, the same computer program that predicts the unexpected results also predicts very reasonable results for the cases in which the shear speed in the solid is low (e.g., lead). Nevertheless, these results are sufficiently surprising that, even with the validity test provided by the energy conservation law, one still tends to be skeptical.

An attempt was made to acquire experimental data to verify the theory. Specifically, reflection and transmission data were acquired for the frequency range 1–5 kHz using both steel and PMM samples. The samples were each square-shaped, 76 cm on a side. The experimental parameters were the same as those used to obtain the theoretical results presented earlier.

These measurements were found to be in reasonably good agreement with simple plane-wave theory and, hence, in apparent disagreement with the predictions of Table I. Insight into the explanation for these negative results can be gained by again referring to Table II. Note that, for the $r' = 100$-cm radius case, the total reflected + transmitted power is 21.3% of the total incident power. However, the $\dot{E}_i(r')$ column shows that only 10.5% of the total incident power actually strikes the relevant circle of observation for this case. This means that if a measurement were carried out using a circularly shaped steel plate of 100-cm radius and 1-cm thickness, quantitative agreement with the predicted results could not possibly occur since, as previously mentioned, much of the power required to create the predicted overpressures originates from portions of the incident wave that would strike the associated infinite plate outside the circle of observation. For quantitative agreement with the theory, a test plate of sufficiently large radius would be required that the total power *actually incident on the test plate* would not differ significantly from the total reflected plus transmitted power passing through the associated circles of observation. [The 250-cm radius case considered in Table II may be a good candidate, since the sum $\dot{E}_r(r') + \dot{E}_t(r')$ exceeds $\dot{E}_i(r')$ by only 2.5% of the total incident power in this instance.] Thus the negative results observed in the measurements described here (which were made using a square-shaped sample having an area[21] less than 20% of that of the 100-cm observation circle of Table II) are most likely a consequence of the very small size of the test sample, and of the data acquisition technique.[22] However, these negative experimental results and the theoretical predictions of Table II

combine to yield an important conclusion regarding panel test measurements: Measurements made on test panels of large cross section may be significantly corrupted by wave-front curvature effects.

The larger the test sample used, the greater the contributions to the observed pressures from panel regions that are far from the receiver. It is clear from Table II that the greater the contributions become from distant panel elements, the greater is the possibility that undesirable wave-front curvature effects will corrupt the results. It is generally desired to obtain the plane-wave response of a test panel. It is also generally believed that panels of large cross section are superior to panels of small cross section for conducting panel tests, since the undesirable influence of panel edge diffraction can be reduced by increasing the panel's lateral dimensions. However, it is clear from the results presented here that the edge-diffraction reduction benefits derived from increasing sample size may be more than offset by the detrimental influences of increased wave-front curvature effects. Of course, this conclusion is based on the assumption that the usual practice of establishing plane-wave conditions by using the farfield of a source is employed. If a suitable array technique is used instead, the spherical-wave effects described here may be suppressed.

It should be noted that the large overpressures predicted here have been only theoretically observed to occur for materials having a shear speed comparable to or greater than the sound speed in the surrounding fluid and that panels are generally fabricated from soft, rubbery materials. It should also be noted that, even for stiff materials, if a sufficiently large loss is present, these overpressures disappear.[23] On the other hand, test panels are frequently fabricated using a steel backing plate for support. It may very well be that, for sufficiently large samples, this steel backing plate introduces undesirable spherical-wave effects into the observations.[24]

IV. SUMMARY AND CONCLUSIONS

The problem of the interaction of a spherical wave with a homogeneous and isotropic solid plate of infinite cross section but finite thickness was considered theoretically. Results of numerical calculations of reflected and transmitted pressure waves for a variety of test materials immersed in a water medium were presented. The theory predicts that when the shear speed in the solid is comparable to or exceeds the sound speed in the surrounding fluid, the reflected- and transmitted-wave pressure amplitudes can exceed the maximum value of the incident-wave pressure amplitude on the surface of the plate. These results are of practical importance to those concerned with acoustical measurements made on planar structures. However, a complete theoretical interpretation of the causes of the results was not presented herein, and this awaits further investigation.

An experiment was performed on polymethylmethacrylate and steel samples using experimental parameters considered in the theoretical calculations. The measurements were found to be in better agreement with simple plane-wave theory than with the spherical-wave calculations presented here. These negative results are very likely a consequence of the very small cross-sectional area of the test samples used. An important conclusion of the present work is that measurements made on test panels of large cross-sectional area may be significantly corrupted by wave-front curvature effects. The practice of using a steel backing plate to support test panels may also introduce undesirable spherical-wave effects into the observations, particularly for samples of large cross section.

[1]The terms "farfield" and "nearfield" are taken here to have the same meaning as previously described in J. C. Piquette, "Spherical wave scattering by an elastic solid cylinder of infinite length," J. Acoust. Soc. Am. **79**, 1248–1259 (1986).

[2]C. B. Officer, *Introduction to the Theory of Sound Transmission* (McGraw-Hill, New York, 1958), pp. 186–248.

[3]J. E. White, *Underground Sound* (Elsevier, New York, 1983), Chap. 6.

[4]L. M. Brekhovskikh, *Waves in Layered Media*, translated by D. Lieberman, and edited by R. T. Beyer (Academic, New York, 1960), Chap. IV.

[5]P. M. Krail and H. Brysk, "Reflection of spherical seismic waves in layered media," Geophysics **48**, 655–664 (1983).

[6]P. M. Morse and K. U. Ingard, *Theoretical Acoustics* (McGraw-Hill, New York, 1968), pp. 638–642.

[7]A. E. H. Love, *A Treatise on the Mathematical Theory of Elasticity* (Dover, New York, 1944), p. 141. To allow for *anelastic* behavior, we follow the usual practice of allowing the material properties to become complex.

[8]The harmonic time dependence $e^{-i\omega t}$ is assumed. For the component resolution of $\nabla^2\mathbf{A}$, see, for example, P. M. Morse and H. Feshback, *Methods of Theoretical Physics* (McGraw-Hill, New York, 1953), p. 116.

[9]See Ref. 6, p. 638.

[10]See Ref. 7, p. 56.

[11]E. Butkov, *Mathematical Physics* (Addison-Wesley, Reading, MA, 1968), p. 694.

[12]F. B. Hildebrand, *Introduction to Numerical Analysis* (McGraw-Hill, New York, 1956), pp. 323–325.

[13]See Ref. 12, pp. 325–327.

[14]See, for example, L. E. Kinsler, A. R. Frey, A. B. Coppens, and J. V. Sanders, *Fundamentals of Acoustics* (Wiley, New York, 1982), pp. 127–131.

[15]Compare Eq. (30) with Eqs. (19) and (20), the solutions for the potentials in the general case.

[16]The material properties used to deduce the results for the metallic cases in Table I were taken from Ref. 14, p. 461. The required properties for the polymethylmethacrylate case were taken from B. Hartmann and J. Jarzynski, "Ultrasonic hysteresis absorption in polymers," J. Appl. Phys. **43**, 4304–4312 (1972).

[17]A. D. Pierce, *Acoustics: An Introduction to Its Physical Principles and Applications* (McGraw-Hill, New York, 1981), p. 40, Eq. 1.11.11b. The referenced equation gives the acoustic intensity. The power integral of Eq. (31) follows from integrating the intensity over the planar surface. The simple area element $2\pi r dr$ is appropriate for angularly independent acoustic fields. The unit vector $\hat{n}$ is equal to $\hat{k}$ on the surface of the plane that faces the source, and is equal to $-\hat{k}$ on the surface of the plane that is opposite the source.

[18]The mechanisms considered were thickness resonances involving longitudinal or shear waves, critical angle phenomena, flexural wave coincidences, and "refraction arrival" phenomena (see Ref. 2, pp. 195–198).

[19]Another possible mechanism, which was not initially considered but was suggested by a reviewer of this article, is the generation of the symmetric Lamb wave by the incident wave. It is possible that such waves may include a component directed toward the origin. These waves would be focused at the origin, and may therefore serve to explain the reported overpressures. However, a thorough investigation of this possibility is beyond the scope and intent of the present article. For a discussion of the physics of the generation of both symmetric and antisymmetric Lamb waves in an elastic plate under plane-wave excitation, the interested reader is directed to R. Fiorito, W. Madigosky, and H. Überall, "Resonance theory of acoustic waves interacting with an elastic plate," J. Acoust. Soc. Am. **66**, 1857–1866 (1979).

[20]See, for example, Ref. 17, p. 128, Eq. (3-5.8), and the discussion in the paragraph following this equation. Although this equation is strictly valid only for thin plates, the computed coincidence frequencies are sufficiently

different from the frequencies of interest that this consideration is not important here.

[21]The tendency exhibited by the values presented in Table II is for the total power propagating away from the plate through the circles of observation, $\dot{E}_r(r') + \dot{E}_i(r')$, to exceed that which is incident on the circle of observation that is facing the source, $\dot{E}_i(r')$, by an increasing percentage for decreasing values of r'. Thus, the smaller the test sample used, the smaller is the likelihood that the predicted overpressures will be observed.

[22]The data acquisition technique involved the use of pulsed interrogating waves and the use of an observation "gate." This gate eliminated contributions to the observed waves originating from the sample edges.

[23]The results presented in Table I for polymethylmethacrylate include loss. Thus the loss factor of this material is insufficient to eliminate the predicted phenomenon, given a sufficiently large sample. It should also be noted that, even though the overpressures disappear when a sufficiently large loss is introduced, the significant differences between plane-wave and spherical-wave theory persist.

[24]Of course, the damping influence of the lossy materials affixed to the steel backing plate may inhibit the spherical-wave effects. This is currently an unresolved issue that must be answered by further research.

SUPPLEMENTARY

INFORMATION

ERRATA

AD-A196183

REPORT DOCUMENTATION PAGE

Form Approved
OMB No 0704-0188

1. AGENCY USE ONLY (Leave blank)	2. REPORT DATE	3. REPORT TYPE AND DATES COVERED
	November 1988	Journal article

4. TITLE AND SUBTITLE
Erratum: "Spherical-wave scattering by a finite-thickness solid plate, with some implications for panel measurements (JASA 83, 1284-94, Apr 88)

5. FUNDING NUMBERS
Work Unit 59-0589-0-0
Assession #DN220-161

6. AUTHOR(S)
Jean C. Piquette

7. PERFORMING ORGANIZATION NAME(S) AND ADDRESS(ES)
Measurements Branch, Underwater Sound Reference Detach.,
Naval Research Laboratory
P.O. Box 568337
Orlando, FL 32856-8337

8. PERFORMING ORGANIZATION REPORT NUMBER

9. SPONSORING/MONITORING AGENCY NAME(S) AND ADDRESS(ES)
Office of Naval Research
800 N. Quincy St.
Arlington, VA 22217-5000

10. SPONSORING/MONITORING AGENCY REPORT NUMBER

11. SUPPLEMENTARY NOTES
This appeared in the Journal of the Acoustical Society of America Vol. 84 (5) page 1939, Nov 1988. It is an erratum for the article appearing in Volume 83 (4) which has AD #A196 183.

12a DISTRIBUTION/~~AVAILABILITY~~ STATEMENT
Approved for public release; distribution unlimited

12b. DISTRIBUTION CODE

13. ABSTRACT (Maximum 200 words)
Same as on original article (AD #A196 183)

14. SUBJECT TERMS
Same as on original article (AD #A196 183)

15. NUMBER OF PAGES
1

16. PRICE CODE

17. SECURITY CLASSIFICATION OF REPORT	18. SECURITY CLASSIFICATION OF THIS PAGE	19. SECURITY CLASSIFICATION OF ABSTRACT	20. LIMITATION OF ABSTRACT
Unclassified	Unclassified	Unclassified	SAR

GENERAL INSTRUCTIONS FOR COMPLETING SF 298

The Report Documentation Page (RDP) is used in announcing and cataloging reports. It is important that this information be consistent with the rest of the report, particularly the cover and title page. Instructions for filling in each block of the form follow. It is important to ***stay within the lines*** to meet ***optical scanning requirements***.

Block 1. Agency Use Only *(Leave blank)*.

Block 2. Report Date. Full publication date including day, month, and year, if available (e.g. 1 Jan 88). Must cite at least the year.

Block 3. Type of Report and Dates Covered. State whether report is interim, final, etc. If applicable, enter inclusive report dates (e.g. 10 Jun 87 - 30 Jun 88).

Block 4. Title and Subtitle. A title is taken from the part of the report that provides the most meaningful and complete information. When a report is prepared in more than one volume, repeat the primary title, add volume number, and include subtitle for the specific volume. On classified documents enter the title classification in parentheses.

Block 5. Funding Numbers. To include contract and grant numbers; may include program element number(s), project number(s), task number(s), and work unit number(s). Use the following labels:

C	- Contract	**PR**	- Project
G	- Grant	**TA**	- Task
PE	- Program Element	**WU**	- Work Unit Accession No.

Block 6. Author(s). Name(s) of person(s) responsible for writing the report, performing the research, or credited with the content of the report. If editor or compiler, this should follow the name(s).

Block 7. Performing Organization Name(s) and Address(es). Self-explanatory.

Block 8. Performing Organization Report Number. Enter the unique alphanumeric report number(s) assigned by the organization performing the report.

Block 9. Sponsoring/Monitoring Agency Name(s) and Address(es). Self-explanatory.

Block 10. Sponsoring/Monitoring Agency Report Number. ***(If known)***

Block 11. Supplementary Notes. Enter information not included elsewhere such as: Prepared in cooperation with...; Trans. of...; To be published in.... When a report is revised, include a statement whether the new report supersedes or supplements the older report.

Block 12a. Distribution/Availability Statement. Denotes public availability or limitations. Cite any availability to the public. Enter additional limitations or special markings in all capitals (e.g. NOFORN, REL, ITAR).

- **DOD** - See DoDD 5230.24, "Distribution Statements on Technical Documents."
- **DOE** - See authorities.
- **NASA** - See Handbook NHB 2200.2.
- **NTIS** - Leave blank.

Block 12b. Distribution Code.

- **DOD** - Leave blank.
- **DOE** - Enter DOE distribution categories from the Standard Distribution for Unclassified Scientific and Technical Reports.
- **NASA** - Leave blank.
- **NTIS** - Leave blank.

Block 13. Abstract. Include a brief *(Maximum 200 words)* factual summary of the most significant information contained in the report.

Block 14. Subject Terms. Keywords or phrases identifying major subjects in the report.

Block 15. Number of Pages. Enter the total number of pages.

Block 16. Price Code. Enter appropriate price code *(NTIS only)*.

Blocks 17. - 19. Security Classifications. Self-explanatory. Enter U.S. Security Classification in accordance with U.S. Security Regulations (i.e., UNCLASSIFIED). If form contains classified information, stamp classification on the top and bottom of the page.

Block 20. Limitation of Abstract. This block must be completed to assign a limitation to the abstract. Enter either UL (unlimited) or SAR (same as report). An entry in this block is necessary if the abstract is to be limited. If blank, the abstract is assumed to be unlimited.

circular segment [Fig. 1(d)], and this effect increases with an increase in the value of r_1/r_0, which makes the segment flatter, approaching a rectangle as shown in Fig. 3 for the case of three azimuthal partitions ($m = 3$).

III. CONCLUDING REMARKS

The foregoing study indicates the following.

(1) One azimuthal partition does not raise the cutoff frequency (the smallest cut-on frequency) at all.

(2) Azimuthal partitioning can at best (for three azimuthal partitions) raise the cutoff frequency parameter ($k_{r,m,n} r_0$) from 1.84 to 3.83.

(3) Provision of a radial partition, in addition, is counterproductive because it lowers the cutoff frequency parameter in the outer annular segments.

The last observation is indeed fortuitous inasmuch as it would be extremely difficult to locate loudspeakers in the inner segments of the duct in an active noise control system.[1]

Finally, it may be pointed out that in the foregoing analysis, the wall and the partitions of the duct have been assumed to be sufficiently massive and rigid, otherwise there would be sound–structure interaction altering the results of the investigation. Besides, the role of damping has also been neglected altogether. In any case viscous damping would have only a marginal effect on the cut-on frequencies of higher order modes.

ACKNOWLEDGMENTS

The author would like to thank the authorities of the Indian Institute of Science for the sabbatical leave that made this investigation possible. His discussions with his colleagues Larry J. Eriksson and Mark C. Allie were very rewarding.

[1] L. J. Eriksson and M. C. Allie, J. Acoust. Soc. Am. Suppl. 1 **80**, S11 (1986).
[2] J. M. Tyler and T. G. Sofrin, SAE Trans. **70**, 309–322 (1962).
[3] C. L. Morfey, J. Sound Vib. **1**, 60–87 (1964).
[4] C. J. Moore, J. Sound Vib. **62**, 235–256 (1979).
[5] M. L. Munjal, *Acoustics of Ducts and Mufflers* (Wiley, New York, 1987), Chap. 1.
[6] L. J. Eriksson, J. Acoust. Soc. Am. **68**, 545–550 (1980).

ERRATUM

Erratum: "Spherical-wave scattering by a finite-thickness solid plate, with some implications for panel measurements" [J. Acoust. Soc. Am. 83, 1284–1294 (1988)]

Jean C. Piquette
Naval Research Laboratory, Underwater Sound Reference Detachment, P. O. Box 568337, Orlando, Florida 32856-8337

(Received 5 July 1988; accepted for publication 28 July 1988)

PACS numbers: 43.20.Fn, 43.30.Gv, 43.10.Vx

Equation (17) was erroneously printed twice in this article, while Eq. (18) was omitted. Equation (18) should have been

$$p_t = \int_0^\infty \frac{b(\beta) J_0(\beta r) \exp\left[j\sqrt{k^2 - \beta^2}(z' - z)\right]}{\sqrt{k^2 - \beta^2}} \beta \, d\beta. \tag{18}$$